Molecular Biology of the Cell
Vol. 18, 2322–2335, June 2007

RKIKK Motif in the Intracellular Domain Is Critical for Spatial and Dynamic Organization of ICAM-1: Functional Implication for the Leukocyte Adhesion and Transmigration[D] [V]

Hyun-Mee Oh,* SungGa Lee,* Bo-Ra Na,* Hyun Wee,* Sang-Hyun Kim,† Suck-Chei Choi,‡ Kang-Min Lee,§ and Chang-Duk Jun*‖

*Department of Life Science, and ‖Research Center for Biomolecular Nanotechnology, Gwangju Institute of Science and Technology, Gwangju 500-712, Korea; †Department of Pharmacology, Kyungpook National University, Daegu 700-422, Korea; ‡Digestive Disease Research Institute, Wonkwang University School of Medicine, Iksan, Chonbuk 570-749, Korea; and §Division of Biological Sciences, College of Natural Science, Chonbuk National University, Jeonju, Chonbuk 561-756, Korea

Submitted August 24, 2006; Revised March 28, 2007; Accepted April 2, 2007
Monitoring Editor: Yu-li Wang

No direct evidence has been reported whether the spatial organization of ICAM-1 on the cell surface is linked to its physiological function in terms of leukocyte adhesion and transendothelial migration (TEM). Here we observed that ICAM-1 by itself directly regulates the de novo elongation of microvilli and is thereby clustered on the microvilli. However, truncation of the intracellular domain resulted in uniform cell surface distribution of ICAM-1. Mutation analysis revealed that the C-terminal 21 amino acids are dispensable, whereas a segment of 5 amino acids (^{507}RKIKK^{511}) in the NH-terminal third of intracellular domain, is required for the proper localization and dynamic distribution of ICAM-1 and the association of ICAM-1 with F-actin, ezrin, and moesin. Importantly, deletion of the ^{507}RKIKK^{511} significantly delayed the LFA-1–dependent membrane projection and decreased leukocyte adhesion and subsequent TEM. Endothelial cells treated with cell-permeant penetratin-ICAM-1 peptides comprising ICAM-1 RKIKK sequences inhibited leukocyte TEM. Collectively, these findings demonstrate that ^{507}RKIKK^{511} is an essential motif for the microvillus ICAM-1 presentation and further suggest a novel regulatory role for ICAM-1 topography in leukocyte TEM.

INTRODUCTION

Leukocyte extravasation across the endothelial barrier is critical for immune surveillance: it is also a fundamental requirement in a wide variety of physiological and pathological situations including immunity and inflammation (Springer, 1994). This phenomenon depends on a stepwise adhesion cascade coordinated by the sequential ligand recognition of cell adhesion molecules expressed on the leukocytes and endothelium (Carlos and Harlan, 1994). At least three steps have been demonstrated: selectin-mediated rolling, β_2 integrin–mediated leukocyte adhesion, and migration across endothelium. Initial rolling is mediated by selectin/glycosylated ligand interactions. The subsequent arrest and adhesion strengthening of leukocytes on the endothelium is mediated by integrins with an Ig superfamily (IgSF) of adhesion molecules on endothelial cells. Morphological changes of leukocytes then accompany the transmigration of leukocytes through the endothelial cell barrier (Springer, 1994).

Over the last few years, leukocyte responses to integrin engagement have been studied extensively, whereas the responses of endothelial cells have received much less attention. However, it has become evident that in addition to enabling leukocytes to adhere to endothelium, adhesion molecules are also involved in the initiation of intracellular signaling systems. In addition, leukocyte migration through endothelium is known to be associated with alterations in the functional state of endothelium, e.g., expression of surface proteins, secretion of cytokines, and increased permeability to macromolecules. These responses are coupled with intracellular modifications including cytoskeletal rearrangement, protein phosphorylation, and calcium influx (Male *et al.*, 1994).

ICAM-1 is a member of the IgSF of adhesion molecules, which is barely detectable in normal endothelial cells, but its expression is enhanced on endothelial cells in response to inflammatory cytokines such as tumor necrosis factor alpha (TNF-α), IL-1β, and IFN-γ (Dustin and Springer, 1988). Antibodies to ICAM-1 inhibit leukocyte adhesion to endothelial cells, granulocyte migration through endothelium, and mitogen and Ag-induced lymphocyte proliferation (Smith *et al.*, 1988, 1989). Crystal structures have been determined for domains 1–2 (D1–D2) and 3–5 (D3–D5) of ICAM-1

This article was published online ahead of print in *MBC in Press* (http://www.molbiolcell.org/cgi/doi/10.1091/mbc.E06–08–0744) on April 11, 2007.

[D] [V] The online version of this article contains supplemental material at *MBC Online* (http://www.molbiolcell.org).

Address correspondence to: Chang-Duk Jun (cdjun@gist.ac.kr).

Abbreviations used: EPI, epifluorescence; ERM, ezrin/radixin/moesin; ERMBMP, ERM-binding membrane proteins; HUVECs, human umbilical vascular endothelial cells; IgSF, Ig superfamily; PBL, peripheral blood lymphocyte; TEM, transendothelial migration.

(Casasnovas *et al.*, 1998; Yang *et al.*, 2004), respectively, and the binding mechanism of ICAM-1 to its receptor, LFA-1, has been characterized in great detail (Jun *et al.*, 2001a,b; Shimaoka *et al.*, 2003).

In addition to the important role of the extracellular domain of ICAM-1, the intracellular domain also plays a pivotal role in leukocyte transendothelial migration (TEM), but has no catalytic activity (Sans *et al.*, 2001; Greenwood *et al.*, 2003). After ICAM-1 cross-linking or coculture with leukocytes, endothelial ICAM-1 initiates intracellular calcium flux and cytoskeletal signal transduction events, including activation of Rho GTPase and phosphorylation of cortactin, paxillin, p130^{cas}, and focal-adhesion kinase (Durieu-Trautmann *et al.*, 1994; Etienne *et al.*, 1998; Adamson *et al.*, 1999; Thompson *et al.*, 2002). Leukocyte TEM is inhibited after the inactivation of endothelial cells' Rho protein function (Adamson *et al.*, 1999), thereby suggesting a proactive role for ICAM-1 signaling/cytoskeletal interactions in facilitating TEM. In agreement with these lines, the intracellular domain of ICAM-1 can bind to a variety of molecules, such as α-actinin (Carpen *et al.*, 1992), β-tubulin, GAPDH (Federici *et al.*, 1996), and ezrin (Heiska *et al.*, 1998). These proteins all have the potential to perform signaling functions. In addition, several reports have described that the deletion of intracellular domain of ICAM-1 abolishes T-lymphocyte migration (Greenwood *et al.*, 2003) as well as PMN migration (Sans *et al.*, 2001).

Despite these extensive studies, however, it is still not clearly delineated whether or not the intracellular domain directly affects the spatial organization and distribution of ICAM-1 on the membrane. Moreover, the linkage between the surface topography of ICAM-1 and its functional consequence in leukocyte TEM has not been determined. To answer these questions, we engineered stable COS-7 cell lines expressing various mutant ICAM-1-GFP proteins whose entire or a part of their intracellular domain was deleted; we then directly visualized them using live time-lapse epifluorescence (EPI) and confocal microscopy. We were able to describe the physical distribution as well as the temporal distribution dynamics of ICAM-1 on live cells existing with or without LFA-1 engagement. This strategy also allowed us to overcome the problem of the multiple adhesion receptors found on endothelial cells.

Recent reports have demonstrated that ICAM-1/LFA-1 or VCAM-1/VLA-4 interactions promote formation of endothelial projections that surround adherent lymphocytes and are enriched in ICAM-1, VCAM-1, ezrin, and actin (Barreiro *et al.*, 2002; Carman *et al.*, 2003). High-resolution imaging study has also suggested that this structure may function to facilitate and guide TEM by forming a cuplike traction structure called a "transmigratory cup" that is aligned parallel to the direction of transmigration (Carman and Springer, 2004). These studies were intriguing and raised the question of what specific site(s) in the intracellular domain is/are responsible for such transmigratory cup formation in the context of leukocyte/endothelial interactions. We found that ^{507}RKIKK^{511} residues in the NH-terminal third of the intracellular domain are required for ICAM-1 membrane projection in response to binding LFA-1 on leukocytes. Accordingly, cell-permeant peptide comprising RKIKK sequences dramatically reduced leukocyte TEM. Importantly, we also found that ^{507}RKIKK^{511} is an essential motif for the microvillus presentation of ICAM-1. The present results imply a novel regulatory role for ICAM-1 topography in leukocyte TEM.

MATERIALS AND METHODS

Cell Culture

COS-7 cells (ATCC CRL-1651, Manassas, VA) were grown in DMEM medium supplemented with 10% heat-inactivated fetal bovine serum (FBS), penicillin G (100 IU/ml), streptomycin (100 μg/ml), and L-glutamine (2 mM). Human umbilical vascular endothelial cells (HUVECs) were isolated from two to five umbilical cord veins, pooled, and established as primary cultures in a complete endothelial growth medium (EGM; Cambrex Bioscience, Baltimore, MD) supplemented with 2% FBS, bovine brain extract (BBE), hEGF, hydrocortisone, and gentamicin. Human peripheral blood lymphocytes (PBLs) were isolated from normal donors by dextran sedimentation followed by centrifugation through a discontinuous Ficoll gradient (Amersham Biosciences, Little Chalfont, England). All the cell lines or primary cells mentioned above were cultured at 37°C in a humidified incubator containing 5% CO_2 and 95% air.

Antibodies and Reagents

Antibody to human ICAM-1 (R6.5) was purified from R6.5 hybridoma (ATCC HB-9580), and anti-GFP was purchased from Santa Cruz Biotechnology (Santa Cruz, CA). CBR-LFA1/2 mAb was kindly provided by Dr. T. A. Springer (Center for Blood Research, Boston, MA). R-phycoerythrin (PE) or fluorescein isothiocyanate (FITC)-conjugated anti-mouse IgG and Phalloidin-TRITC were purchased from Sigma (St. Louis, MO). Monoclonal anti-ezrin and anti-moesin were acquired from BD Biosciences (San Diego, CA), and Cy5-conjugated anti-mouse IgG was from Molecular Probes (Eugene, OR). Polyclonal anti-phospho ERM (pERM) and anti-ezrin were purchased from Cell Signaling Technology (Beverly, MA). Horseradish peroxidase–conjugated anti-mouse IgG was purchased from Amersham Biosciences. Anti-ICAM-1 (CBR IC1/11) Fab was prepared by papain cleavage using the ImmunoPure Fab Preparation kit (Pierce, Rockford, IL) according to the manufacturer's instructions. Conjugation of anti-ICAM-1 Fab to Cy-3 bisfunctional dyes (Amersham Pharmacia Biotech, Piscataway, NJ) was also performed by the manufacturer's instruction manual. Human TNF-α, SDF-1α, and anti-pECAM-1 antibody were purchased from R&D Systems (Minneapolis, MN). Lipofectamine 2000 reagent was from Invitrogen (Carlsbad, CA). Small interfering RNA (siRNA) targeting ezrin and a scrambled siRNA were obtained as a pool of four or more siRNA duplexes from Dharmacon (Chicago, IL).

Recombinant DNA Constructs

The human wild-type ICAM-1/pAprM8 was kindly provided by Dr. T. A. Springer. To generate the various deletion mutants of ICAM-1, a PCR amplification was performed using human wild-type ICAM-1/pAprM8 as a template and the following primers: a sense primer for all mutants (5′-AGGATC-C^{1}ATGGCTCCCAGCAGC^{15}-3′) containing the BamHI restriction site and an antisense primer for IC1ΔCTD (5′-AGCGGCCGC^{1512}GTTATAGAGGTACG-TGCT-G^{1494}-3′), IC1Δ509-532 (5′-AGCGGCCGC^{1524}CTTCCGCTGGCGGTT-ATAG^{1506}-3′), IC1Δ517-532 (5′-AGCGGCCGC^{1548}CTGTTGTAGTCTGTATT-TCTTG^{1527}-3′), and IC1Δ521-532 (5′-AGCGGCCGC^{1560}CCCTTTTTGGGC-CTGTTGTA-G^{1540}-3′) containing the NotI restriction site, respectively. IC1ΔRKIKK cDNA was generated by an overlapping PCR. In the first PCR reaction, using wild-type ICAM-1/pAprM8 as a template, a 1530-base pair fragment was generated from the sequences of starting codon to the sequences of the 11th codon of the intracellular domain without the internal RKIKK amino acids. Using ICAM-1/pAprM8 as a template, a 94-base pair fragment was also generated. This encodes the last C-terminal amino acids (YNRQYRLQQAQKGTPMKPNTQATPP) of ICAM-1 followed by a stop codon and a NotI site. In the final PCR reaction, the 1530- and 94-base pair products were used together as an overlapping template to generate an IC1ΔPKIKK. The PCR products were then subcloned as BamHI/NotI fragments into a pEF1/V5-His-puro (Invitrogen) vector in which the neomycin-resistant gene was replaced by puromycin.

ICAM-1/pEGFP-N1 was obtained using the corresponding ICAM-1/pEF1/V5-His-puro as templates by PCR amplification of the complete or partial encoding region of the molecule without the stop codon. A HindIII site was added to the 5′ end and a SacII site at the end of wt-IC1 and IC1ΔRKIKK cDNAs. Likewise, NheI and HindIII sites were added to the 5′ and 3′ ends of the ICAM-1 mutants. The PCR products were subcloned into pEGFP-N1 (CLONTECH Laboratory, Palo Alto, CA), resulting in an in-frame fusion of enhanced green fluorescent protein (GFP) to the COOH terminus of ICAM-1. The amino acid sequences of a linker polypeptide between wt-IC1 or IC1ΔRKIKK protein and the EGFP residues, were GDPPVAT (7 aa). In the case of C-terminal deletion mutants, we inserted more linker polypeptide in order to adjust a sequence length as in the cytoplasmic domain, thereby overcoming a potential localization problem. The amino acid sequences of a linker polypeptide between mutant ICAM-1s and EGFP, were KLRILQSTVDRARDPPVAT (19 aa).

To generate wild-type ezrin (wt-ezrin) construct, human ezrin clone coding for the full-length open reading frame of ezrin was purchased from RZPD German Resource Center (Berlin, Germany). Wt-ezrin cDNA was then transferred into the pcDNA3 vector (Invitrogen) using EcoRI and XhoI restriction sites. Wt-ezrin_RFP was generated using PCR amplification from wt-ezrin/

pcDNA3, and subcloned into the pDsRed1-N1, thereby resulting in an in-frame fusion of RFP to the COOH terminus of wt-ezrin. DN-ezrin$_{1-320}$/pEGFP-N1 was a generous gift from Dr. Stephenie M. Takahashi (National Institutes of Health, Bethesda, MD). DN-ezrin$_{1-320}$ was transferred into pDsRed1-N1 vector (CLONTECH Laboratory) to produce DN-ezrin_RFP construct.

PECAM-1/pcDNA3 was kindly provided by Dr. Peter J. Newman (Blood Research Institute, Milwaukee, WI). To generate PECAM-1 fused to GFP at its C terminus, the stop codon of PECAM-1 was replaced with an EcoRI restriction site through the PCR amplification of the entire coding region of PECAM-1. The resultant PCR product was digested with HindIII and EcoRI and subcloned into the pEGFP-N1 vector (CLONTECH Laboratory), thus giving rise to the plasmid PECAM-1/pEGFP-N1.

Cell Transfection and Establishment of Stable Cell Lines

COS-7 cells were transiently transfected with cDNAs encoding wild-type or mutant ICAM-1s using the Lipofectamine 2000 reagent (Invitrogen) according to the manufacturer's instructions. In some experiments, COS-7 cells were transiently cotransfected with ICAM-1 and wt-ezrin_RFP or DN-ezrin_RFP and then used for the localization studies at 24–48 h after transfection.

For siRNA transfections, COS-7 cells were treated for 48 h with 1 μg of siRNA targeting ezrin or a scrambled siRNA premixed with DharmaFECT 2 according to the manufacturer's instructions. The cells were then retransfected with wt-ICAM-1_GFP for 24 h and the effect of siRNA on the expression of ezrin was examined by immunofluorescence staining analysis.

Stable COS-7 transfectants were established using the Lipofectamine 2000 reagent (Invitrogen) transfection of ICAM-1/pEGFP-N1 or ICAM-1/pEF1 V5 His-puro, followed by selection with 1 mg/ml geneticin or 3 μg/ml puromycin (Invitrogen, Gaithersburg, MD), respectively. The cells were then subjected to a fluorescence-activated cell sorter (FACS) and were sorted in order to obtain ICAM-1–positive cells selectively; they were then cultured in complete medium supplemented with the same concentrations of antibiotics.

HUVECs were transiently transfected with cDNAs encoding wild-type or mutant ICAM-1s using a Nucleofector device and corresponding kits (Amaxa, Cologne, Germany). HUVECs were harvested at days 3 or 4 of culture, washed once in cold phosphate-buffered saline, and resuspended in the specified electroporation buffer to a final concentration of 2.5×10^5 cells/0.1 ml. Two micrograms of plasmid DNA was mixed with 0.1 ml of cell suspension, transferred to a 2.0-mm electroporation cuvette, and nucleofected with an Amaxa Nucleofector apparatus (Amaxa, Cologne, Germany) according to the manufacturer's instructions. After electroporation, cells were immediately transferred to 5.0 ml of complete medium and cultured in six-well plates at 37°C until analysis.

Penetratin-ICAM-1 Peptides

Penetratin peptides were N-terminally biotinylated and consisted of 16 residues of the penetratin sequence (RQIKIWFQNRRMKWKK) as previously described (Greenwood *et al.*, 2003). The 14 C-terminal or ^{507}RKIKK^{511} amino acids of human ICAM-1 were synthesized distal to the penetratin sequence. The sequences used for ICAM-1 were RQRKIKKYRLQQAQ, RKIKK, and an irrelevant sequence was from the soluble part of rat rod opsin (CKPMSNFRFGENH). Peptides were HPLC-purified before use. Localization of penetratin peptides was detected in cells using streptavidin-Texas red after fixation in 3.7% formaldehyde and permeabilization with 0.2% Triton X-100.

Immunofluorescence Staining and Confocal Imaging Analysis

Cells (COS-7 transfectants or HUVECs) were grown on glass coverslips (18-mm diameter; Fisher Scientific, Pittsburgh, PA) or on chamber slides (Nalge Nunc International, Naperville, IL). HUVECs were treated for various times (0–12 h) with TNF-α (10 ng/ml). The cells were fixed, washed twice with PBS, and blocked with 5% goat serum (DAKO, Glostrup, Denmark) in PBS for 30 min. The cells were then incubated with primary antibodies in blocking buffer for 3 h at RT, rinsed three times with PBS, incubated with secondary antibody in blocking buffer for 1 h at RT, rinsed three times with PBS, and mounted with anti-fade solution (Molecular Probes). The primary antibodies used were anti-ICAM-1 (R6.5), anti-ezrin, anti-moesin, and anti-pERM; the secondary antibodies used were Cy5-conjugated goat anti-mouse and anti-rabbit IgG (Molecular Probes). F-actin was detected using Phalloidin-TRITC (Sigma). To stain the ERM protein family, cells were permeabilized for 5 min with PBS containing 0.1% Triton X-100 at RT before incubation with primary antibody. The slides were examined with an FV1000 confocal laser scanning microscope (Olympus, Tokyo, Japan) equipped with 40×, 63×, and 100× objectives.

For the colocalization analysis, the *Z* section cutting area through the apical surface was chosen. Images captured at different wavelengths were superimposed, and the intensity of expression for each fluorochrome in the field was then plotted in a scattergram by FLUOVIEW software (Olympus). Overlapping degree of intensity (ODI) value was calculated by FLUOVIEW software. Colocalization percentage was then derived from the ODI, multiplying by 100.

For measuring microvilli length, images captured were traced using the free line tool bar on FLUOVIEW software and were analyzed by measurement analysis. Microvilli in 8–10 cells were calculated for the measurement of microvilli length.

Flow Cytometric Analysis

Single-cell suspensions obtained after EDTA (5 mM/PBS) treatment were collected by centrifugation and were washed once in PBS containing 1% bovine serum albumin (BSA). The cells were resuspended in 1% BSA/PBS for 30 min on ice. For extracellular staining, the cells were then incubated with ICAM-1 antibody (R6.5) for 1 h on ice, washed once with 1% BSA/PBS, and incubated with PE or FITC-conjugated anti-mouse IgG for 1 h on ice. After two further washes with 1% BSA/PBS, samples were analyzed and quantified using the FACScan cell analyzer (Becton Dickinson, San Jose, CA). Appropriate isotype-matched Ab controls were used in each experiment. Cells for sorting were incubated as described above and were then sorted on an FACSAria (Becton Dickinson, San Jose, CA) machine equipped with a 5-W argon and a 30-mW helium neon laser. Sorted cells were collected into sterile Eppendorf vials in complete medium.

Immunoprecipitation and Western Blotting

Cells (COS-7 transfectants) were lysed in ice-cold lysis buffer (50 mM Tris-HCl, pH 7.4, containing 150 mM NaCl, 1% Nonidet P-40, 0.1% SDS, 0.1% deoxycholate, 5 mM sodium fluoride, 1 mM sodium orthovanadate, 1 mM 4-nitrophenyl phosphate, 10 μg/ml leupeptin, 10 μg/ml pepstatin A, and 1 mM 4-(2-aminoethyl)benzenesulfonyl fluoride) for 1 h on ice. Cell lysates were centrifuged at 15,000 rpm for 20 min at 4°C, and the supernatant was incubated with R6.5-bead conjugates at 4°C overnight with rotation. Immune complexes were then washed in lysis buffer, eluted with SDS sample buffer (100 mM Tri-HCl, pH 6.8, 4% SDS, 20% glycerol with bromophenol blue), and heated for 5 min. The proteins were separated through 8–10% SDS-PAGE gels and were transferred into a nylon membrane by means of Trans-Blot SD semidry transfer cell (Bio-Rad, Hercules, CA). The membrane was blocked in 5% skim milk (1 h), rinsed, and incubated with intended antibodies (anti-GFP, anti-ezrin, and anti-ICAM-1 antibodies) in TBS containing 0.1% Tween 20 (TBS-T) and 3% skim milk for 2 h. Excess primary antibody was then removed by washing the membrane four times in TBS-T. The membrane was then incubated with 0.1 μg/ml peroxidase-labeled secondary antibody (against rabbit or mouse) for 1 h. After three washes in TBS-T, bands were visualized by ECL Western Blotting Detection reagents and were then exposed to x-ray film.

Live-Cell, Time-Lapse Confocal, and EPI Fluorescence Imaging

For live-cell time-lapse confocal imaging, COS-7 cells expressing wt-IC1, IC1ΔCTD, or IC1ΔRKIKK (with or without GFP form) were seeded at 2×10^5 on 18-mm glass coverslips. After overnight culture, the coverslips were mounted in a chamber device. In some experiments, PBLs (1×10^6 cells/coverslip) were added on the COS-7 cells (Supplementary Figure S4B and Figure 7). PBLs were allowed to settle for 10 min at 37°C and were then activated by adding CBR-LFA-1/2 antibody. During the live-cell imaging, chamber devices were maintained at 37°C in a 5% CO_2 atmosphere using a live-cell instrument system (Live Cell Instrument, Inc., Seoul, Korea). Confocal series of fluorescence and differential interference contrast (DIC) images were simultaneously obtained at 20-s intervals using an 63× oil immersion objective on FV1000 confocal microscope (Olympus). The images were processed and assembled into movies using Olympus FLUOVIEW software ver.1.5.

For EPI fluorescence imaging, cells transfected with wt-IC1_GFP were prepared as described above. Live-time EPI fluorescence and DIC images were taken at 30-s intervals with a 40× objective in an Axiovert 200 fluorescence microscope (Carl Zeiss, Jena, Germany). Images were analyzed using Axiovision software ver. 3.1 (Zeiss).

Scanning Electron Microscopy

COS-7 cells expressing WT-IC1 or IC1ΔCTD in pEF1/V5-His-puro were analyzed by scanning electron microscopy (Model S-4800, Hitachi, Tokyo, Japan). The cells were seeded on 18-mm glass coverslips. After overnight culture, the coverslips were fixed in a solution of 4% formaldehyde and 2% glutaraldehyde in PBS overnight at 4°C. The cells were then washed twice with 0.1 M cacodylate buffer, dehydrated in graded ethanol, and air-dried at room temperature. The cells on coverslips were mounted on SEM stubs with double-sided carbon tape, and were then coated gold-palladium in a vacuum evaporator. The cells were observed and photographed with SEM operated at 10 kV.

Understatic Adhesion and Transmigration Assays

For cellular adhesion assays, stable COS-7 cells (1×10^5 cells/well) or HUVECs (5×10^4 cells/well) were grown to confluence in 96-microwell plates (Costar, Pittsburgh, PA). HUVECs were stimulated for 12 h with TNF-α (10 ng/ml) and were then treated for 2 h with penetratin-ICAM-1s (100

μg/ml) before use. PBLs (2×10^5 cells/200 μl) were labeled with 1 μM of BCECF-AM for 15 min at 37°C, preincubated with CBR-LFA-1/2 antibody (for adhesion assay on COS-7 cells only), and allowed to adhere to the bottom cells in Lefkovitz L15 media supplemented with 5% FBS (L15/5% FBS) for 30 min at 37°C. Unbound PBLs were then removed and the fluorescence intensity was measured in a microplate reader (FL500, Biotek, Winooski, VT).

PBL migration through a confluent monolayer of stable COS-7 transfectants or TNF-α–stimulated HUVECs was assayed in 3-μm pore Transwell cell culture chambers (Costar). Stable COS-7 transfectants (1×10^5 cells/well) expressing wild-type or mutant ICAM-1s or HUVECs (1×10^5 cells/well) were seeded and grown to confluence on these Transwell inserts. HUVECs were further treated with TNF-α and penetratin-ICAM-1s as described above. In the low chamber, 600 μl of complete medium with or without 100 ng/ml human SDF-1α, were poured before PBL was added into the upper chamber. Cells were incubated for 3 h at 37°C, and migrated cells were recovered from the lower chamber. The relative number of migrated cells was estimated by flow cytometry.

Underflow Adhesion and Migration Assays

Stable COS-7 transfectants (2×10^5) were seeded on 22-mm glass coverslips, grown to confluence, and then preincubated with SDF-1α (100 ng/ml) for 10 min. Coverslips were mounted in a flow chamber device and maintained at 37°C in a 5% CO_2 atmosphere as described on live-cell time-lapse imaging. For underflow adhesion and detachment assays, PBLs were resuspended at 2×10^6/ml in L15/5% FBS, loaded into the chamber under shear stress at 0.2 dyn/cm^2 for 5 min, and then subjected to a constant shear force of 4 dyn/cm^2 for 15 min. In some experiments, the shear force was increased up to 20 dyn/cm^2 for 10 min after the initial shear force of 0.2 dyn/cm^2 for 5 min and 4 dyn/cm^2 for 5 min. The number of cells attached after shear stress was quantified by a direct visualization of six to eight different fields (40× oil immersion objective). For underflow migration assay, the behaviors of PBLs on the monolayers of COS-7 transfectants at 4 dyn/cm^2 were monitored on confocal microscopy by obtaining DIC images at 20-s intervals (40×–60× oil immersion objective). Images were analyzed using Olympus FLUOVIEW software ver. 1.5.

HUVECs (2×10^5) were also seeded on 22-mm glass coverslips, grown to confluence, and then pretreated with TNF-α (10 ng/ml) for 12 h. The cells were further incubated with penetratin-ICAM-1 peptides for 2 h and washed three times with serum-free medium (EGM). To visualize ICAM-1 on plasma membrane, HUVECs were then treated with Cy3-conjugated anti-ICAM-1 Fab (CBR-IC1/11-Fab-Cy3) for 10 min after treatment with SDF-1α (100 ng/ml). The PBL adhesion and migration assays were performed as described in COS-7 transfectants. Confocal series of fluorescence and DIC images were simultaneously obtained at 20-s intervals with 40×–63× oil immersion objective lens in an FV1000 confocal microscope, and images were analyzed as described above. The PBLs that remained firmly adherent were scored for adhesion. The PBLs that randomly migrated on the monolayers of endothelial cells were scored for migration. The PBLs that underwent shape changes to flattened morphology together with the redistribution of ICAM-1 on HUVECs were scored for transmigration. The number of adhered, migrated, and transmigrated PBLs was counted by a direct visualization of six to eight randomly selected fields (40× oil immersion objective), respectively, and the total number of cells in each field was considered as 100%. The results are expressed as the percent adhesion, migration (lateral), and transmigration of binding PBLs in each field.

Online Supplementary Material

Supplementary Figure S1 shows the localization of wild-type ICAM-1 or ICAM-1 mutant lacking an intracellular domain on the surface of primary HUVECs. Supplementary Figure S2 shows that pERM is localized on the tip of growing microvilli in COS-7 cells expressing wt-IC1_GFP. Supplementary Figure S3 shows that activation of HUVECs by TNF-α induces ICAM-1 and microvillar elongation. Supplementary Figure S4 shows the dynamic movement of ICAM-1 clusters on the surface of COS-7 wt-IC1_GFP cells. Supplementary Videos 1 and 2 (corresponding to Figure 1, C and D, respectively) show a microvillus redistribution of wt-IC1_GFP or IClΔCTD_GFP at the marginal zone of cells. Supplementary Video 3 (corresponding to Supplementary Figure S4A) shows a continuous and directional movement of wt-IC1_GFP clusters on the cell surface by EPI fluorescence. Supplementary Video 4 (corresponding to Supplementary Figure S4B) shows a clustering of wt-IC1_GFP in the interface between PBLs and COS-7 cells. Supplementary Video 5 (corresponding to Figure 7A) shows a 3D view of ICAM-1–mediated membrane projection upon binding to LFA-1 on leukocytes. Supplementary Videos 6 and 7 (corresponding to Figure 7B) show membrane projections mediated by wt-IC1_GFP (Supplementary Video 6) and IC1ΔRKIKK_GFP (Supplementary Video 7). Supplementary Videos 8 and 9 (corresponding to Figure 8) show leukocyte binding to and migration on monolayers of COS-7 cells that express wt-IC1 (Supplementary Video 8) or IC1ΔRKIKK (Supplementary Video 9) in a parallel wall flow chamber. Supplementary Videos 10 and 11 (corresponding to Figure 10C) show leukocyte binding to and migration through the monolayers of TNF-α/SDF-1α–activated HUVECs that were pretreated with penetratin-ICAM-1s.

RESULTS

The Distribution and Dynamic Movements of ICAM-1 on Transfected COS-7 Cells

To directly visualize the distribution and dynamic movements of ICAM-1 on the cell surface, we generated COS-7 cells that transiently or stably express ICAM-1 fused to GFP (wt-IC1_GFP). We also generated COS-7 cells that express the ICAM-1 lacking intracellular domain (C-terminal 28 amino acids; IC1ΔCTD_GFP) in order to investigate potential function of intracellular domain on the distribution and localization of ICAM-1. Although earlier studies have utilized the CHO cell system to overcome the problem of multiple adhesion receptors found on endothelial cells (Sans *et al.*, 2001; Carman *et al.*, 2003), others have found that Chinese hamster ovary (CHO) cells express endogenous cell surface molecules that mediate T-cell costimulation (Gaglia *et al.*, 2001). We also noticed that this uncharacterized molecule could mediate T-cell adhesion potentially through its interaction with LFA-1 (data not shown).

We first examined the cell surface distribution of the two forms of ICAM-1 using confocal microscopy and flow cytometry. Wt-IC1_GFP was most prominent of the microvillar projections on the membrane surface, and this was strongly colocalized with the signals detected by the anti-ICAM-1 antibody (R6.5; Figure 1A, left). The majority of IC1ΔCTD_GFP, on the other hand, was uniformly distributed on the cell membrane (Figure 1A, left). Because both proteins were well expressed on the cell surface, as evidenced by the surface staining of the anti-ICAM-1 antibody in flow cytometric analysis (Figure 1B), uniform distribution of IC1ΔCTD_GFP may not result from improper expression. To rule out the possibility that the fusion of ICAM-1 with GFP by itself alters the distribution of ICAM-1 on the cell surface, COS-7 cells were also transfected with ICAM-1 constructs without GFP and were stained with anti-ICAM-1 antibody. No significant difference was detected between the cells that express ICAM-1 with and without GFP (Figure 1A, right), thereby suggesting that GFP has little effect on the expression and distribution of ICAM-1 on the cell surface. Time-lapse microscopic analysis revealed that wt-IC1_GFP is condensed to the newly formed microspikes at the marginal zone of the cells, whereas IC1ΔCTD_GFP barely shows condensed distribution (Figure 1, C and D; see Supplementary Videos 1 and 2). To further test whether the results from COS-7 were applicable to the endothelial cells, we examined the cell surface distribution of the wt-IC1_GFP and IC1ΔCTD_GFP on HUVECs. As shown in Supplementary Figure S1, the physical distributions of two forms of ICAM-1 on HUVECs were similar to that of COS-7 cells.

Earlier reports have demonstrated that native ICAM-1 protein is associated with the actin-containing microfilament network and that their interaction is mediated by the cytoplasmic or transmembrane domains of ICAM-1 (Carpen *et al.*, 1992; Carman *et al.*, 2003). ICAM-1 has also been known to be associated with ezrin/radixin/moesin (ERM) family members, i.e., ezrin and moesin (Heiska *et al.*, 1998; Barreiro *et al.*, 2002). To test whether truncation of the intracellular domain alters the association of ICAM-1 with the proteins mentioned above, the subcellular distribution of ICAM-1, actin, ezrin, and moesin was analyzed by confocal microscopy in COS-7 cells transfected with wt-IC1_GFP or IC1ΔCTD_GFP. Wild-type ICAM-1 colocalized with F-actin, ezrin, and moesin in the microspikes and microvilli that protrude from the apical surface of these cells (Figure 2, A–C). Colocalization scattergram analysis also confirmed these observations (Figure 2, A–C). In contrast, ICAM-1

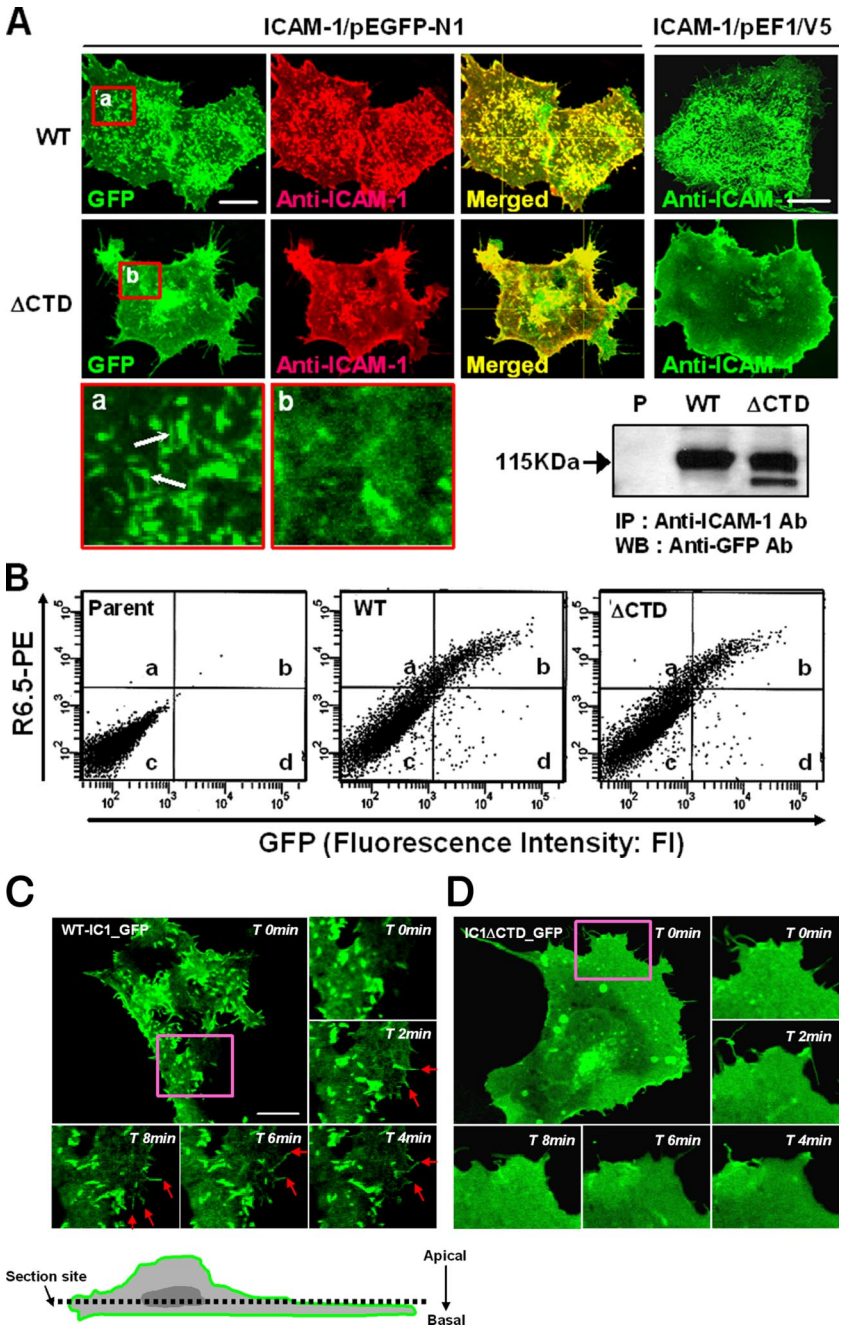

Figure 1. Characterization of COS-7 cell lines that were transfected with cDNAs containing wild-type ICAM-1 or ICAM-1–lacking intracellular domain. (A) Immunofluorescence staining and confocal imaging of COS-7 cells expressing wild-type ICAM-1 (wt-IC1 in pEGFP-N1 = wt-IC1_GFP; wt-IC1 in pEF1/V5-His-puro = wt-IC1) or ICAM-1–lacking intracellular domain (IC1ΔCTD in pEGFP-N1 = IC1ΔCTD_GFP; IC1ΔCTD in pEF1/V5-His-puro = IC1ΔCTD). Cells were fixed and stained with anti-ICAM-1 (R6.5) mAbs (10 μg/ml), followed by incubation with TRITC- or FITC-conjugated secondary antibody, as described in *Materials and Methods*. Cells were imaged using confocal microscopy with reconstitution in the *z*-axis. To determine the expression and folding of ICAM-1s fused with GFP protein, the cell lysates were immunoprecipitated with R6.5 mAb and were then blotted with HRP-conjugated anti-GFP antibody (bottom). Bars, 10 μm. (B) Flow cytometric analysis of ICAM-1 expression on COS-7 cells. (C and D) Time-lapse confocal microscopic analysis of ICAM-1-GFP proteins expressed on COS-7 cells. The distribution of wt-IC1_GFP (C) or IC1ΔCTD_GFP (D) was followed for 10 min by time-lapse confocal microscopy at 37°C. Selected images are shown at 0, 2, 4, 6, and 8 min of culture from a representative experiment (see also Supplementary Videos 1 and 2). Arrowheads indicate the high intensity of the GFP signals at the newly formed microspikes in the marginal zone of cells in the COS-7 wt-IC1_GFP cells. Bars, 10 μm.

lacking an intracellular domain revealed reduced colocalization with F-actin and with the ERM family (Figure 2, A–C). Taken together, these results demonstrate that the intracellular domain is critical for the proper localization of ICAM-1 on the microvilli, presumably by its interaction with F-actin and ERM proteins.

The Intracellular Domain of ICAM-1 Involves in Microvillar Organization and F-Actin Formation

It has been previously demonstrated that some ERM-binding membrane proteins (ERMBMP), such as CD43, CD44, and ICAM-2, are directly involved in the organization of microvilli (Yonemura and Tsukita, 1999). Because ICAM-1 also has been known to associate with ezrin and moesin (Carpen *et al.*, 1992; Barreiro *et al.*, 2002), we therefore tested whether the overexpression of ICAM-1 by itself directly induces microvillar elongation in COS-7 cells. As shown in Figure 3A, the elongation of microvilli as well as F-actin formation, were significantly increased in cells that express higher levels of ICAM-1, as determined by flow cytometry and confocal analysis. The length of microvilli in cells expressing a low level of wt-IC1_GFP (box 1 in Figure 3A), was usually shorter than 1 μm (0.49 $\pm$ 0.25 μm; n = 50), whereas in cells expressing middle or high levels of wt-IC1_GFP (boxes 2 and 3 in Figure 3A), most microvilli were 2–3 μm in length (1.98 $\pm$ 0.31 and 3.46 $\pm$ 0.66 μm, respectively; n = 50). These results are comparable with those in villin-induced (2.5 μm; Friederich *et al.*, 1989) or ERMBMP-induced (3–4 μm; Yonemura and Tsukita, 1999) microvilli. We also examined the surface morphology of these cells by scanning

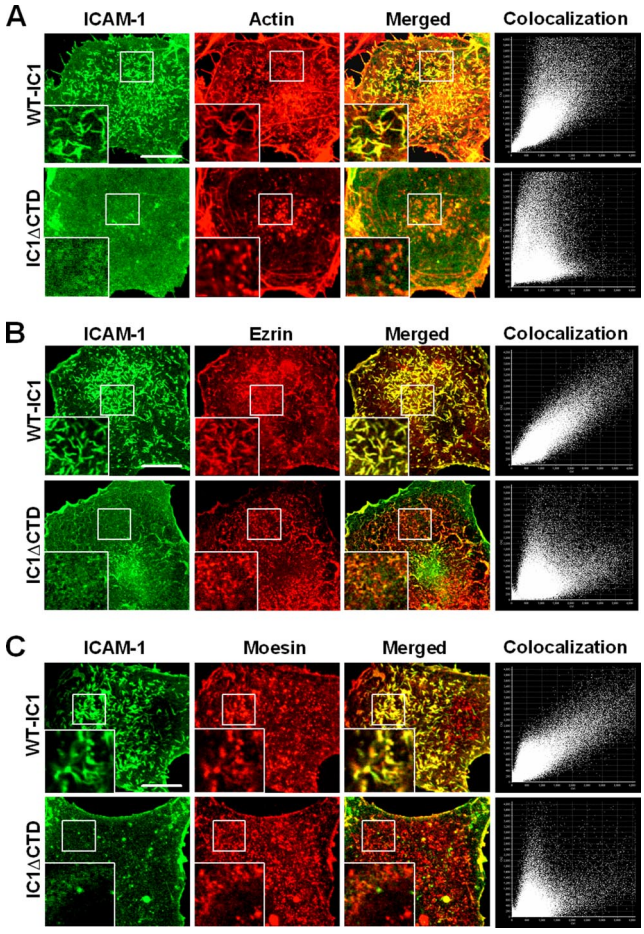

Figure 2. ICAM-1 is colocalized with F-actin, ezrin, and moesin in microvilli. COS-7 cells expressing wt-IC1_GFP or IC1ΔCTD_GFP were fixed and stained with TRITC-phalloidin (A) or with anti-ezrin (B) or anti-moesin (C) antibodies, followed by incubation with the cy5-conjugated secondary antibody. The cells were then imaged using confocal microscopy with reconstitution in the *z*-axis. Insets represent a magnified single image of the serial *Z*-sections. Colocalization dot plots corresponding to these images are shown on the right. The corresponding colocalization percentages are 84.8% (WT) and 27.4% (ΔCTD) for F-actin, 92.1% (WT) and 46.4% (ΔCTD) for ezrin, and 87.5% (WT) and 33.2% for moesin, respectively. Bars, 10 μm.

electron microscopy (Figure 3B). The surface of COS-7 wt-IC1_GFP cells was characterized by numerous, elongated microvilli as well as by microspikes on the apical surface of these cells. In contrast, only a small number of short microvilli were observed on the surface of IC1ΔCTD_GFP-transfected cells (Figure 3B). Interestingly, the phospho-type of ERMs (pERM) was mostly localized on the tip of growing microvilli in COS-7 wt-IC1_GFP (Supplementary Figure S2). This result may suggest that microvillar protrusion is initiated on the apical side of microvilli. Similar results were also observed when HUVECs were treated with TNF-α (10 ng/ml; Supplementary Figure S3, A and B). In these cells, the microvillar elongation was also highly dependent on the expression levels of ICAM-1, as determined by confocal microscopic imaging (Supplementary Figure S3, A and B) and by flow cytometric analysis (Supplementary Figure S3C).

Because ERM proteins have been thought to play a central role in the organization of the microvillar formation (Yonemura and Tsukita, 1999), we therefore questioned whether the targeted inhibition of ERM action alters the ICAM-1–induced microvilli formation in COS-7 cells. We first examined the action of dominant negative ezrin (DN-ezrin_RFP) in COS-7 cells by cotransfecting with the wt-IC1_GFP. DN-ezrin lacks the F-actin–binding domain. It therefore functions as a dominant-negative mutant by competing with endogenous ERM proteins (Amieva *et al.*, 1999). As shown in Figure 4A, DN-ezrin_RFP dramatically reduced microvilli formation in that cells expressing wt-IC1_GFP. Although wt-ezrin significantly augmented ICAM-1–mediated microvilli formation, it had no influence on IC1ΔCTD localization (Figure 4A). We secondarily examined the effect of siRNA targeted to the ezrin. As shown in Figure 4B, transfection with the siRNA targeting the ezrin significantly reduced the endogenous ezrin expression. Accordingly, it also inhibited ICAM-1–induced microvilli formation in COS-7 cells. Taken together, these results strongly suggest that normal functioning of ezrin is required for the ICAM-1–induced microvillar elongation. To further test whether the microvillar elongation is also mediated by other endothelial membrane proteins, we examined the effect of PECAM-1 (CD31). Transfection of COS-7 cells with the cDNA encoding PECAM-1 (either wild type or GFP-fused form) did not induce the microvilli formation, but rather most cells revealed a uniform distribution of PECAM-1 on the cell surface (Figure 4C).

The RKIKK Motif in the Intracellular Domain Is Critical for the Spatial Organization and Dynamic Behavior of ICAM-1 during Leukocyte Adhesion and Transmigration

To determine which region in the intracellular domain is critical for the spatial distribution of ICAM-1 on the cell surface, we designed a series of ICAM-1 constructs that were truncated parts of the intracellular domain (Figure 5A). Two criteria were applied to design these constructs. First, although it has been known that ICAM-1 has no catalytic activity associated with its intracellular domain, there are potential phosphorylation sites in its internal sequence. Therefore, the first two truncation mutants were designed around ^{521}T residue, thereby generating IC1Δ521-532_GFP and IC1Δ517-532_GFP. Second, as ^{507}RKIKK^{511} of five amino acids in the NH-terminal third of the intracellular domain has been known as an α-actinin–binding motif (Carpen *et al.*, 1992), the last two constructs were designed by deleting all (IC1ΔRKIKK_GFP) or part (IC1Δ509-532_GFP) of the ^{507}RKIKK^{511} residues. All of the mutant ICAM-1s were properly folded and were well expressed on the cell surface, as determined by immunoprecipitation and flow cytometric analysis (Figure 5B, right). Interestingly, however, there were significant differences of their physical distributions on the cell surface. As shown in Figure 5B in the left panel, deletion of the C-terminal 16 amino acids (IC1Δ517-532_GFP) showed no significant effect on the expression and localization of ICAM-1 on the microvilli compared with wild-type ICAM-1. In contrast, deletion of all (ΔRKIKK) or the C-terminal 24 amino acids, including ^{509}IKK^{511} residues (Δ509-532), revealed uniform distribution of ICAM-1 on the cell surface. Moreover, both constructs (IC1ΔRKIKK_GFP and IC1Δ509-532_GFP) failed to induce F-actin formation, which represented a weak association with F-actin (Figure 5C). In addition, deletion of the ^{507}RKIKK^{511} residues revealed reduced colocalization with ezrin and moesin (data not shown).

We therefore questioned whether the ICAM-1 interaction with ERM is directly or indirectly altered by RKIKK mutation in COS-7 cells. To overexpress ezrin, COS-7 cells ex-

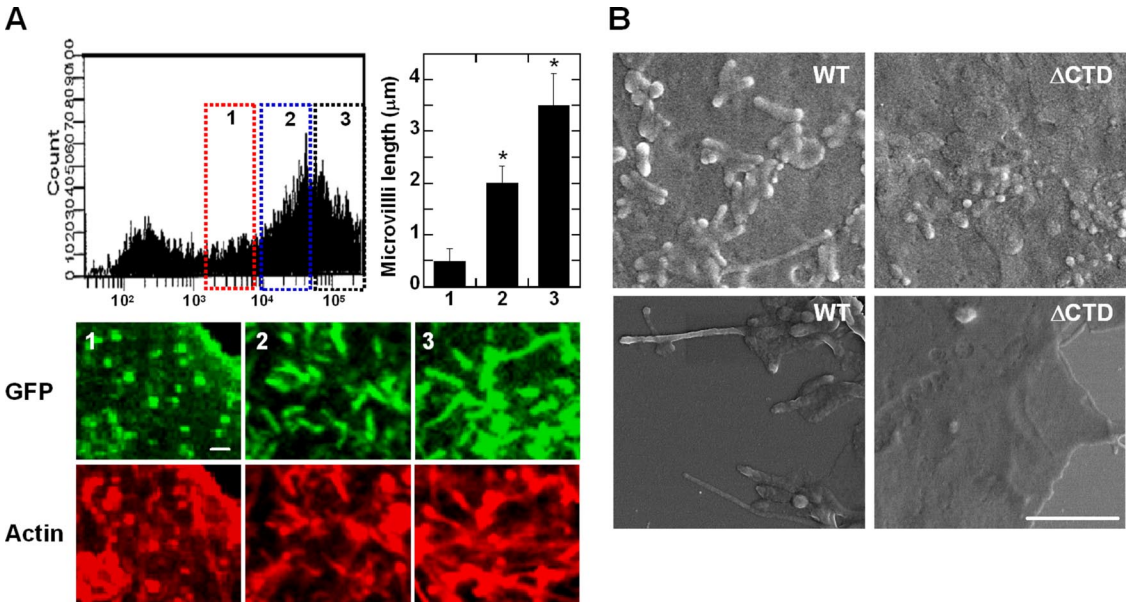

Figure 3. ICAM-1 induces microvillar elongation in COS-7 cells. (A) Overexpression of ICAM-1 induces F-actin and microvillar elongation. COS-7 cells were transiently transfected with 1 μg of plasmid producing wild-type ICAM-1 fused to GFP protein. The cells were subdivided to the three groups, i.e., 1, low; 2, medium; and 3, high, based on their GFP intensity, and were then stained with TRITC-phalloidin (bottom). Bottom, selected Z-stack confocal sections showing F-actin and microvillar elongation associated with the expression levels of ICAM-1. Right graph, quantification of microvilli length by using the FLUOVIEW software ver.1.5. Values correspond to the arithmetic mean ± SD of a representative experiment of three independent ones. *$p < 0.01$, significantly different from GFP-transfected cells ($n = 3$). Bar, 1 μm. (B) COS-7 cells expressing WT-IC1 or IC1ΔCTD in pEF1/V5-His-puro were analyzed by scanning electron microscopy as described in *Materials and Methods*. Bar, 2.5 μm.

pressing wt-IC1, IC1ΔCTD, and IC1ΔRKIKK were transfected with cDNA containing wt-ezrin. As shown in Figure 6, wt-IC1 was coimmunoprecipitated with ezrin, whereas both IC1ΔCTD and IC1ΔRKIKK were not coimmunoprecipitated with ezrin. Taken together, these results strongly suggest that RKIKK is a critical motif for the interaction of ICAM-1 with the ERM proteins.

The significant differences between wild-type ICAM-1 and ICAM-1 lacking RKIKK motif in terms of their spatial distribution on the cell surface led us to ask whether these molecular topographies were linked to the functional consequence of ICAM-1. Because no report has been demonstrated the distribution dynamics of ICAM-1 clusters in microvilli, by using time-lapse EPI microscopy, we initially observed the dynamic behavior of wt-IC1_GFP signals on the cell surface in the absence or presence of leukocyte binding. As shown in Supplementary Figure S4A (see also Supplementary Video 3), interestingly, wt-IC1_GFP clusters, which appeared as punctuate forms at low resolution, revealed a continuous and directional movement on the cell

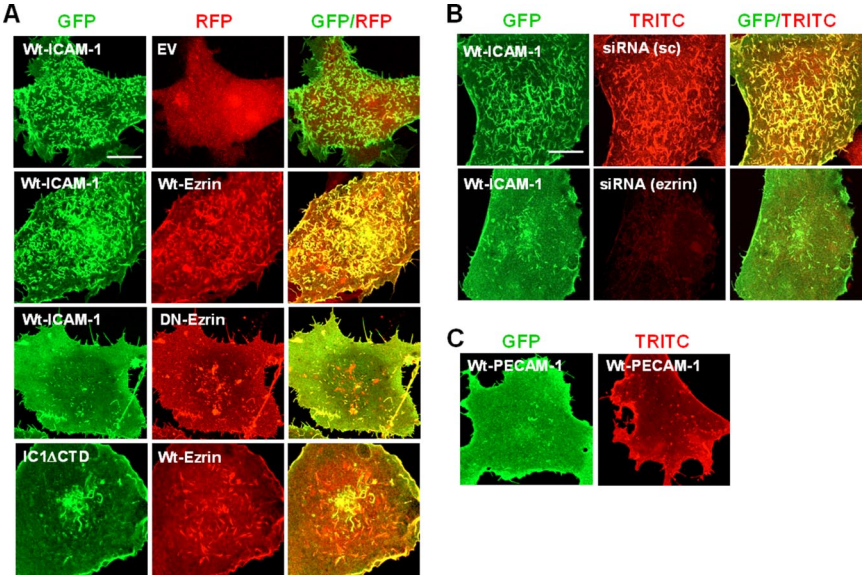

Figure 4. ICAM-1–induced microvillar organization requires ERM activity. COS-7 cells were transfected with the indicated cDNAs (wt-IC1_GFP; Wt-Ezrin in pDesRed = Wt-Ezrin_RFP; DN-Ezrin in pDesRed = DN-Ezrin_RFP; Wt-PECAM-1 in pCDNA3.1 = Wt-PECAM-1; Wt-PECAM-1 in pEGFP-N1 = Wt-PECAM-1_GFP; pDsRed1-N1 = EV) or siRNA targeted ezrin. After 24 h of transfection, the cells were fixed, and the localization of the indicated proteins was analyzed by the confocal microscopy, as described in Figure 3. (A and B) Inhibition of ICAM-1-induced microvillar organization by DN-ezrin (A) and siRNA targeting ezrin (B). sc, scrambled siRNA. (C) PECAM-1 does not induce the microvilli formation. Bars, 10 μm.

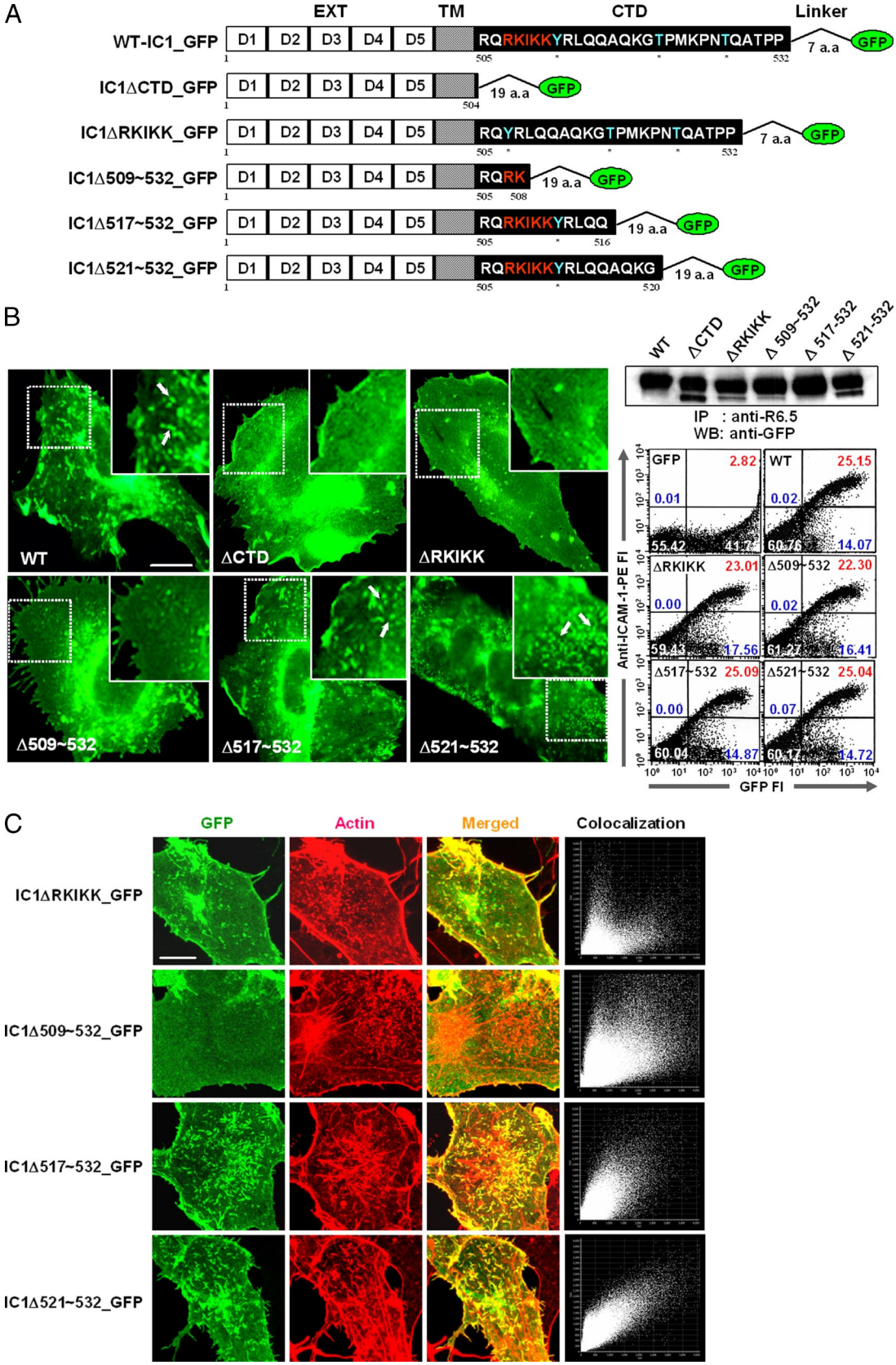

Figure 5. Schematic representation of C-terminally mutated ICAM-1-GFP constructs and their expression on the surface of cells. (A) Wild-type and mutant ICAM-1 proteins fused to GFP. IgSF domains 1–5 (EXT), transmembrane domain (TM), intracellular domain (CTD), linker, and GFP are indicated by the white, shaded, black boxes, line, and green circle, respectively. The putative phosphorylation sites and α-actinin–binding site are colored by cyan and red, respectively. (B) EPI fluorescence imaging of the COS-7 transfectants expressing

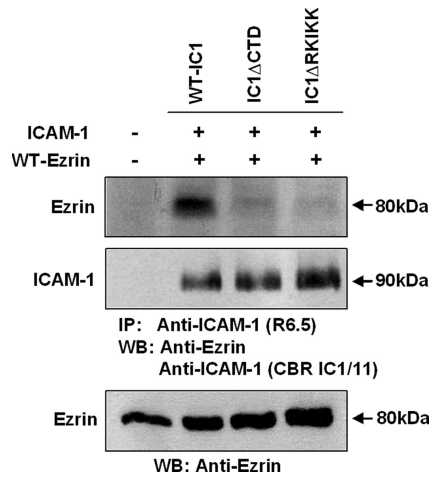

Figure 6. Association of ezrin with the RKIKK motif of ICAM-1. COS-7 cells (1×10^7) expressing wt-IC1, IC1ΔCTD, or IC1ΔRKIKK were transfected with the cDNA encoding wt-ezrin. Cells were lysed and immunoprecipitated with the R6.5-bead conjugates. Immunoprecipitates were then resolved on a 8% SDS-PAGE and sequentially immunoblotted with the anti-ICAM-1 mAb (CBR IC1/11) and the anti-ezrin mAb. Parent cells were used as a negative control. To evaluate the transfection efficiency, lysates of ezrin-transfected cells were also immunoblotted with the anti-ezrin mAb. Molecular weights (KD) are indicated on the right side.

surface during the imaging time (~25 min), although this was not observed in IC1ΔRKIKK_GFP-expressing cells (data not shown). In addition, upon binding to LFA-1 on leukocytes, these clusters were rapidly redistributed and formed a ringlike cluster at the leukocyte–endothelial junctional interface (Supplementary Figure S4B; see Supplementary Video 4). As ICAM-1 clusters in microvilli are not static but are actively moving on the cell surface, it also suggests the importance of the intracellular domain in the spatial and physical dynamics of ICAM-1.

Recently, as shown in Figure 7A (see also Supplementary Video 5), several reports have demonstrated that ICAM-1 and activated moesin and ezrin are rapidly clustered in an endothelial actin-rich docking structure during leukocyte adhesion onto endothelial cells (Barreiro *et al.*, 2002; Carman *et al.*, 2003; Carman and Springer, 2004). We found that the ability of each construct to support leukocyte adhesion in the presence of CBR-LFA-1/2 mAb (activation antibody) was similar to that of wild-type ICAM-1, as measured by under static adhesion assay (see Figure 8A). Nevertheless, the velocity to form a ring-shaped membrane projection in response to binding to LFA-1 on human PBLs, was significantly more retarded in cells expressing mutant ICAM-1s lacking the RKIKK motif (IC1ΔCTD_GFP, IC1ΔRKIKK_GFP, and IC1Δ509-532_GFP) than in cells expressing wild-type ICAM-1 (wt-IC1_GFP) or mutant ICAM-1s with the RKIKK motif (IC1Δ521-532_GFP and IC1Δ517-532_GFP), as measured by time-lapse confocal microscopy (Figure 7B; see Supplementary Videos 6 and 7). As a consequence, the number of ring-shaped projections per cell was also reduced in cells expressing mutant ICAM-1s lacking the RKIKK motif (Figure 7C). Overall, compared with the cells expressing ICAM-1s with the RKIKK motif, the percent of ring-shaped projection formed by binding with the LFA-1–bearing cells was significantly diminished in the cells expressing ICAM-1 lacking the RKIKK motif (Figure 7D).

We also assessed the capacity of COS-7 cells expressing various ICAM-1 mutants to support leukocyte adhesion and transmigration under the static flow condition. Basal binding of leukocytes was significantly increased by activation with mAb CBR-LFA1/2 (Figure 8A) and was reduced by ICAM-1 and LFA-1 blocking mAbs to the levels similar to those exhibited by untreated leukocytes (data not shown). The ability of COS-7 cells expressing various ICAM-1 mutants to support leukocyte adhesion was similar to that of wt-IC1 (Figure 8A). In contrast, leukocyte transmigration across COS-7 IC1ΔCTD, IC1ΔRKIKK, and IC1Δ509-532 in response to chemokine SDF-1α was significantly reduced compared with that of COS-7 wt-IC1 (Figure 8B).

To more preciously evaluate whether the results from the above static adhesion assay are applicable to the physiological shear flow condition, we characterized PBL binding to and migration on monolayers of COS-7 cells that express wt-IC1 or IC1ΔRKIKK in a parallel wall-flow chamber. For this experiment, we used ICAM-1 constructs without GFP to reduce a potential effect of the GFP protein. PBLs were accumulated on SDF-1α–pretreated mono-layers of COS-7 wt-IC1 or COS-7 IC1ΔRKIKK mounted on the bottom wall of the flow chamber for 5 min at 0.2 dyn/cm^2 and then subjected to a constant shear force of 4 dyn/cm^2 for 15 min. To further test whether PBL binding on COS-7 expressing ICAM-1 mutants is also resistant to detachment under increasing shear stress, the shear force was increased up to 20 dyn/cm^2 (10-fold more than physiological shear stress) for 10 min after the initial shear force at 0.2 dyn/cm^2 for 5 min and 4 dyn/cm^2 for 5 min. The initial binding of leukocytes to the monolayers of COS-7 IC1ΔRKIKK was not significantly different from that of COS-7 wt-IC1 in terms of the number of bindings per cell under shear force at 0.2 dyn/cm^2 (data not shown). In addition, little change of leukocyte adhesion was observed under shear force at 4 dyn/cm^2 (Figure 9A). Interestingly, however, there was a slight but significant reduction of leukocyte adhesion on the monolayers of COS-7 IC1ΔCTD, IC1ΔRKIKK, and IC1Δ509-532 under shear force at 20 dyn/cm^2 (Figure 9A), thereby suggesting that spatial and physical distribution of ICAM-1 on the cell surface may also affect the avidity of ICAM-1. In addition, most leukocytes that adhered to the COS-7 wt-IC1 underwent shape changes to more flattened morphology and migrated rapidly on or across monolayers during the incubation period. In contrast, leukocytes on COS-7 IC1ΔRKIKK cells remained as round in shape and revealed reduced motilities (Figure 9B; see Supplementary Videos 8 and 9). Taken together, these results strongly suggest that ICAM-1 topography on the cell surface has an important functional consequence in leukocyte-adhesion–induced morphological changes, migration, and transmigration.

Cell-permeant Peptides Comprising the RKIKK Motif Attenuate ICAM-1 Redistribution during Leukocyte Adhesion and Migration and Inhibit TEM of Leukocytes

To further evaluate whether a heterotypic experimental model (COS-7 cells) used in this study is properly applicable

Figure 5 (cont). wt-IC1_GFP (WT), IC1ΔCTD_GFP (ΔCTD), IC1ΔRKIKK_GFP (ΔRKIKK), IC1Δ509–532_GFP (Δ509-532), IC1Δ517-532_GFP (Δ517-532), and IC1Δ521-532_GFP (Δ521-532) (left). The expression and folding of ICAM-1 proteins were determined as described in Figure 1, A and B. (C) Localization of various constructs of ICAM-1-GFP with F-actin in COS-7 cells. Actin staining and confocal microscopic study were performed as shown in Figure 3. The corresponding colocalization percentages are 46.6% (ΔRKIKK), 38.5% (Δ509-532), 74.3% (Δ517-532), and 78.4% (Δ521-532) for F-actin, respectively. Bars, 10 μm.

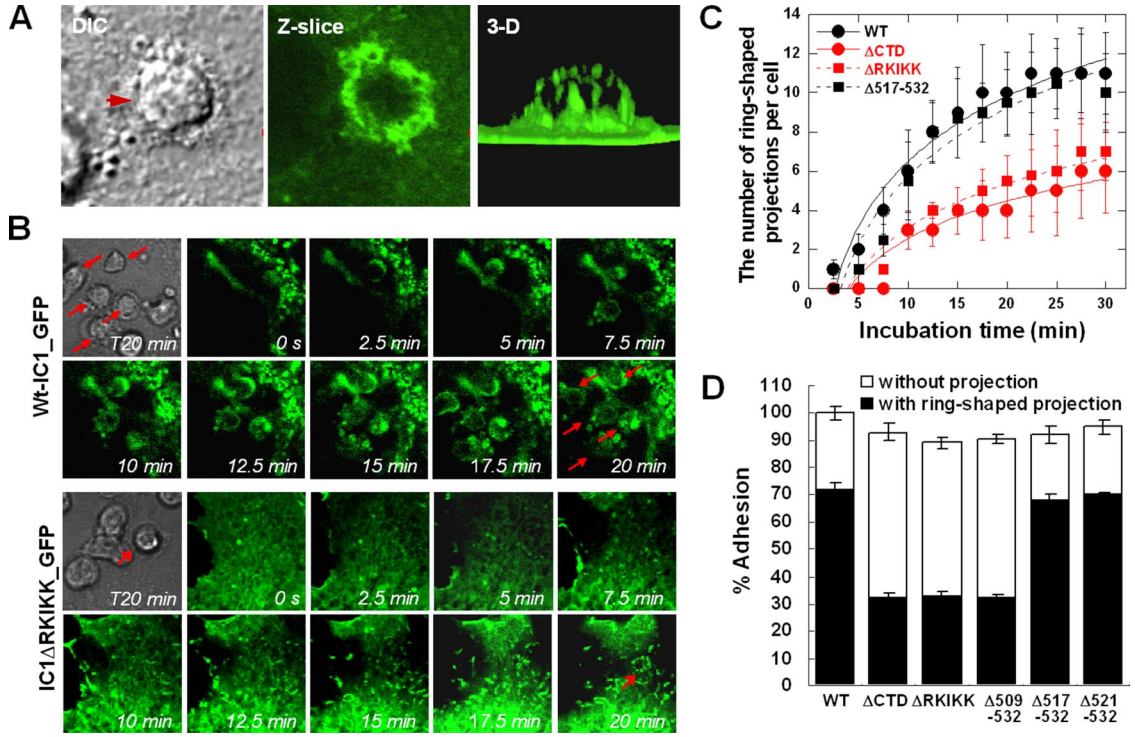

Figure 7. The RKIKK motif is critical for ICAM-1–mediated, ring-shaped membrane projection upon binding to LFA-1 on leukocytes. COS-7 cells expressing wt-IC1_GFP or IC1ΔRKIKK_GFP were incubated with CBR-LFA-1/2 mAb-activated PBMCs for various times and were then imaged by live-cell confocal microscopy. (A) Photos represent selected images of DIC (left), single *Z*-axis slice (middle), and 3D (right; see also Supplementary Video 5). (B) The distribution of wt-IC1_GFP (WT) and IC1ΔRKIKK_GFP (ΔRKIKK) was followed for 20 min by time-lapse confocal microscopy at 37°C. Selected images at 0, 2.5, 5, 7.5, 10, 12.5, 15, 17.5, and 20 min of culture from a representative experiment are shown (see also Supplementary Videos 6 and 7). Arrowheads indicate the ring-shaped membrane projections upon binding to LFA-1 on leukocytes. (C) During the incubation time, selected fields were viewed in all *z*-planes and the presence of ring-shaped projections was scored per one COS-7 cell. At least 1 μm in length was regarded as projection. (D) One hundred adherent cells from randomly selected fields were viewed in all *z*-planes, and the percentage of adhesions with or without ring-shaped projections was calculated as a proportion of the adhesion cells on the COS-7 cells expressing wt-IC1_GFP. Values are the mean ± SD of three experiments (C and D).

to the endothelial cells, we were trying to understand the function of ICAM-1 RKIKK motif in its cellular context, i.e., HUVECs. To this end, peptides comprising the 14 C-terminal amino acids or RKIKK residues were used to antagonize the binding potential of ICAM-1–binding/signal partners. Such ICAM-1 peptides were fused to the penetratin sequence to facilitate the uptake of peptides into cells (Hall *et al.*, 1996; Sans *et al.*, 2001). We assessed the effects of penetratin-ICAM-1 peptides (P-CTD, RQRKIKKYRLQQAQ; P-RKIKK, and RKIKK) for the leukocyte adhesion to and transmigration through HUVECs under the static flow condition. As shown in Figure 10A, treatment with these peptides did not reduce leukocyte adhesion on TNF-α–activated HUVECs. Thus, treatment with either the P-CTD or P-RKIKK resulted in adhesion values 101.2 ± 4 (n = 4) and 98.3 ± 6% (n = 4) of control (TNF-α alone) values, respectively. Interestingly, however, P-CTD and P-RKIKK were both effective in attenuating TEM of leukocytes through monolayers of HUVECs. Both P-CTD and P-RKIKK peptides reduced TEM to 44.2 ± 3 and 51.2 ± 3% of the control value ($p < 0.05$; n = 4), respectively (Figure 10A).

Finally, we tested the leukocyte adhesion on and migration across HUVECs under the shear flow condition. HUVECs were pretreated with TNF-α (10 ng/ml) for 12 h and then treated with penetratin-ICAM-1 peptides for 2 h. To visualize the dynamic distribution of ICAM-1 on endothelial cells, cells were further stained for 10 min with Cy-3–conjugated anti-ICAM-1-Fab (CBR-IC1/11-Fab-Cy3). HUVECs

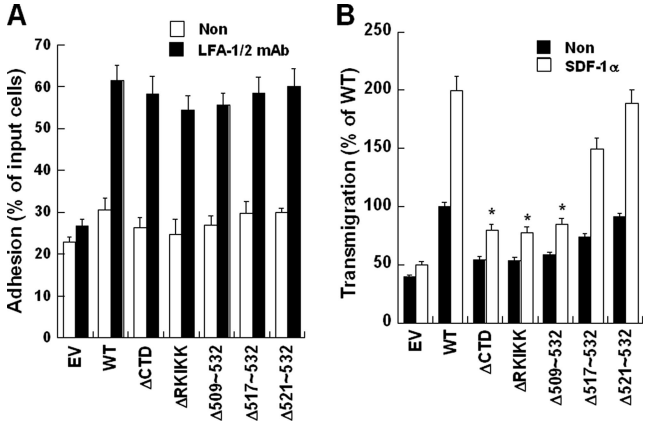

Figure 8. Deletion of RKIKK motif inhibits leukocyte transmigration but not adhesion under static-flow condition. (A) Attachment of human PBLs to COS-7 ICAM-1 mutants under static-flow condition. PBLs were incubated with COS-7 ICAM-1 mutants in the presence or absence of CBR-LFA-1/2 mAb. Adhesion assay was performed for 30 min at 37°C. The results are expressed as the percent adhesion of input PBLs. (B) PBL transmigration across COS-7 cells expressing indicated ICAM-1 proteins was performed in the presence or absence of SDF-1α (100 ng/ml). Results obtained with COS-7 wt-IC1 without SDF-1α treatment was considered as 100%. EV, empty vector (pEF1/V5-His-puro). Transmigration assays were performed as described in *Materials and Methods*. Values are the mean ± SD of three experiments. *$p < 0.05$ versus WT (+SDF-1α).

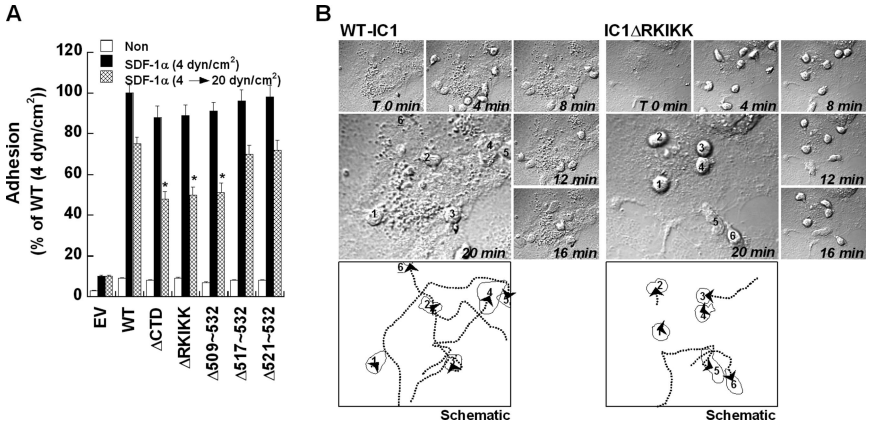

Figure 9. Deletion of RKIKK motif inhibits leukocyte adhesion and transmigration under shear-flow condition. (A) Attachment of human PBLs to COS-7 ICAM-1 mutants under shear-flow condition. PBLs (1×10^6 cells/ml) were incubated with COS-7 transfectants pretreated with or without SDF-1 for 10 min. Shear stress was applied for 5 min at 0.2 dyn/cm^2 and then subjected to a constant shear force of 4 dyn/cm^2 for 10 min. As indicated in the graph, the shear force was also increased up to 20 dyn/cm^2 for 10 min after 4 dyn/cm^2 for 5 min. The result obtained with COS-7 wt-IC1 pretreated with SDF-1α at shear force of 4 dyn/cm^2 was considered as 100%. (B) PBLs (2×10^6 cells/ml) were accumulated on SDF-1α–pretreated (100 ng/ml) monolayers of COS-7 wt-IC1 or COS-7 IC1ΔRKIKK mounted on the bottom wall of the flow chamber for 5 min at 0.2 dyn/cm^2 and then subjected to a constant shear force of 4 dyn/cm^2 shear force for 10 min. Adhesion and migration of PBLs on COS-7 wt-IC1 or IC1ΔRKIKK was followed by time-lapse microscopy at 37°C. Selected images are shown at 0, 4, 8, 12, 16, and 20 min of culture from a representative experiment (see also Supplementary Videos 8 and 9). Numbers indicate the PBLs adhered on COS-7 wt-IC1 or IC1ΔRKIKK. The underlined number stands for the cell that is out of field. In the schematic representation, and dotted lines with an arrowhead in the bottom planes indicate the distance of leukocyte migration after attachment. Solid lines represent the shape of cells adhered on COS-7 cells expressing wt-IC1 or IC1ΔRKIKK.

were washed at least three times with serum-free medium to minimize abnormal clustering of penetratin peptide with antibody at the plasma membrane of cells. In all experiments, HUVECs were incubated with SDF-1 before use (~30 min). We found that P-CTD or P-RKIKK has little effect on the ICAM-1 distribution (Figure 10B) as well as viability (data not shown). Using live-cell time-lapse imaging, we then carefully monitored the behaviors of leukocytes on the HUVECs that were pretreated with penetratin-ICAM-1 peptides. The initial binding of leukocytes was not significantly altered by the treatment with the penetratin-ICAM-1 peptides (data not shown). In control (TNF-α/SDF-1) or irrelevant peptide-treated cells, most leukocytes underwent shape changes to flattened morphology in response to binding on HUVECs during the measuring time (see Supplementary Video 10). Interestingly, in parallel with the shape changes of leukocytes, there were also dynamic redistributions of ICAM-1 on the HUVECs, implying a trans- or para-cellular leukocyte migration (Supplementary Video 10; Carman and Springer, 2004). In contrast to the control (data not shown) or irrelevant peptide-treated cells (Supplementary Video 10), however, many leukocytes were randomly migrated but

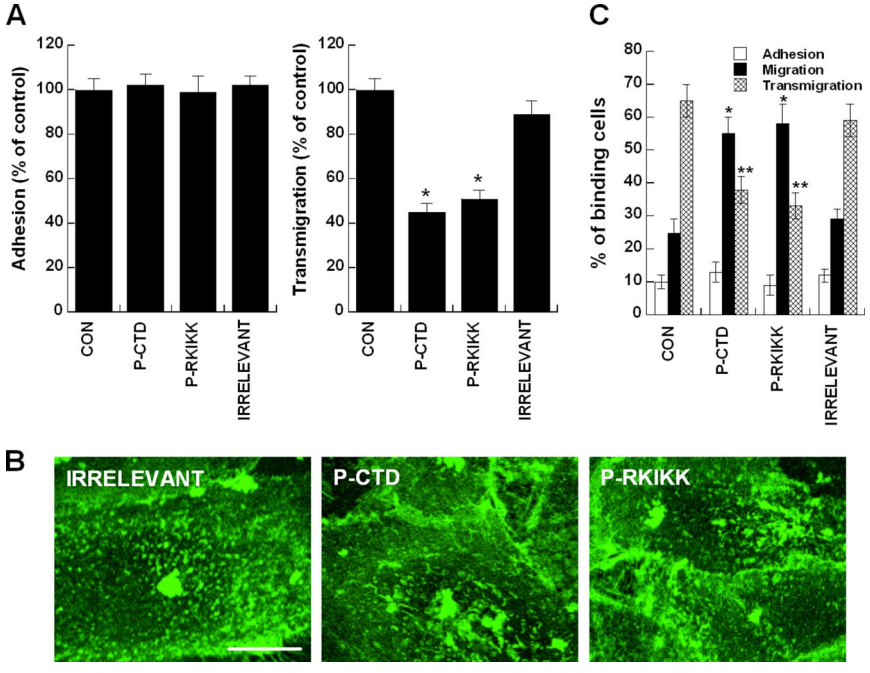

Figure 10. Leukocyte adhesion to and migration through TNF-α/SDF-1α–activated monolayers of endothelial cells in the presence of penetratin-ICAM-1 peptides. (A) Understatic adhesion and transmigration of PBLs. Left, Human PBLs were incubated with TNF-α/SDF-1α–activated monolayers of HUVECs in the presence or absence of indicated penetratin-ICAM-1 peptides (100 μg/ml). Adhesion assay was performed for 30 min at 37°C. Right, PBL transmigration across TNF-α/SDF-1α–activated monolayers of HUVECs was performed in the presence or absence of indicated penetratin-ICAM-1 peptides as described in *Materials and Methods*. Result obtained with HUVECs without penetratin-ICAM-1 peptides was considered as 100%. Values are the mean ± SD of three experiments. *$p < 0.05$ versus control (CON). (B and C) Underflow adhesion and transmigration of PBLs. HUVECs were prepared as described in A. The cells were stained for 10 min with CBR-IC1/11-Fab-Cy3 fragment to visualize the distribution dynamics of ICAM-1 in the presence or absence of penetratin-ICAM-1 peptides. The representing images are shown in B. Underflow adhesion and transmigration assays were performed as described in *Materials and Methods* (C). The results are expressed as the percent adhesion, migration (lateral), and transmigration of binding PBLs in each field (40× oil immersion objective). The number of adhered, migrated, and transmigrated PBLs was counted by a direct visualization of 6–8 randomly selected fields, respectively, and the total number of cells in each selected field was considered as 100%. See also Supplementary Videos 10 and 11. *$p < 0.05$ versus control (migration); **$p < 0.05$ versus control (transmigration).

were not undergone shape changes on the monolayers of HUVECs treated with the P-CTD (data not shown) or P-RKIKK (Supplementary Video 11). Quantitative analysis revealed that treatment with either the P-CTD or P-RKIKK reduced the percentage of transmigration of binding cells (P-CTD, 36.5 ± 4%; P-RKIKK, 32.3 ± 4%), compared with the control group (64.2 ± 5%, $p < 0.05$; $n = 4$; Figure 10C). We also performed a flow chamber assay in the absence of CBR-IC1/11-Fab-Cy3 to rule out a possible influence of antibody fragments on penetratin-treated HUVECs and confirmed that no significant differences were observed in terms of leukocyte behaviors on HUVECs (data not shown). Taken together, our current results strongly suggest that ^{507}RKIKK^{511} is not only involved in the spatial and dynamic organization of ICAM-1 but also participated in the regulation of leukocyte TEM.

DISCUSSION

An intracellular domain of ICAM-1 is required for efficient adhesion and migration of leukocytes across the monolayers of endothelial cells (Sans *et al.*, 2001; Greenwood *et al.*, 2003). However, the molecular details of its action have not been clearly delineated. By using engineered COS-7 cells that express the wild type and varying forms of ICAM-1 fused to GFP, we visualized the spatial organization and distribution dynamics of ICAM-1 on the cell surface and determined a specific region of the intracellular domain that is critical for leukocyte/endothelial interaction and transmigration. We primarily characterized, with high spatial resolution, the morphological and functional differences between two cells expressing wild-type ICAM-1 and ICAM-1 lacking the intracellular domain. Wild-type ICAM-1, which localized in microvilli, revealed a characteristic of continuous directional movement on the surface membrane and was highly colocalized with F-actin, ezrin, and moesin. In contrast, mutant ICAM-1 that deleted the intracellular domain revealed uniform cell surface distribution. Interestingly, induction of wild-type ICAM-1 directly elongated microvilli. We secondarily identified what site(s) in the intracellular domain is/are essentially required for the proper localization as well as the functional consequences of ICAM-1. We found that ^{507}RKIKK^{511} residues, which were previously identified as an α-actinin–binding motif, in the intracellular domain is required for 1) localization of ICAM-1 on the microvilli; 2) association with F-actin, ezrin, and moesin; 3) redistribution of ICAM-1 in a newly formed ring-shaped membrane projection upon binding to LFA-1–bearing leukocytes; 4) supporting adhesion and migration of leukocytes under shear force; and eventually 5) leukocyte TEM. The functional role of RKIKK motif of ICAM-1 was further proved in the endothelial cells, by testing the effects of the penetratin-ICAM-1 peptides.

ICAM-1 appears to exist as a dimer or higher multimers in its native state on the cell surface, as shown by cross-linking studies (Miller *et al.*, 1995; Reilly *et al.*, 1995), and it has been postulated that the multimeric form of ICAM-1 mediates better adhesion to LFA-1. However, the relative importance of the topographical distribution of ICAM-1 in connecting with its function to mediate leukocyte transmigration has been less extensively investigated. Our current results using time-lapse EPI microscopy unambiguously represent that ICAM-1 clusters are not just staying in one place but are moving continuously on the entire membrane surface of cells. On engagement with LFA-1 on leukocytes, these clusters are rapidly joined at the junctional interface of leukocyte/endothelial interactions. As mutant ICAM-1 lacking an intracellular domain did not show any of these features, these results strongly suggest that an intracellular domain is vital for the proper positioning of ICAM-1 on the microvilli through which ICAM-1 may play a pivotal role for leukocyte migration.

It is interesting to note that the expression levels of ICAM-1 correlated with the elongation of microvilli as determined by flow cytometric analysis, confocal microscopy, and scanning electron microscopy. These results suggest that the intracellular domain has an essential motif that is not just for associating with actin but for actively functioning as an organizer for the recruitment of actin filaments, thereby inducing microvillar elongation. In this regard, the question has naturally arisen which site(s) in the intracellular domain is(are) responsible for this event. Our results strongly indicated that the ^{507}RKIKK^{511} residues, which were previously identified as an α-actinin–binding motif (Carpen *et al.*, 1992), play a pivotal role for the microvillar organization and ICAM-1 association with F-actin, ezrin, and moesin. In mutagenesis analysis, deletion of all (ΔRKIKK) or part (Δ509-532) of the ^{507}RKIKK^{511} residues significantly diminishes ICAM-1–dependent microvillar elongation, whereas deletion (Δ517-532 or Δ521-532) of the C-terminal remaining amino acids except for ^{507}RKIKK^{511} has no significant effect. A striking feature of ^{507}RKIKK^{511} residues is the presence of positively charged amino acids. A positively charged amino acid cluster in the juxta-membrane portion has been identified as an ERM protein-binding region in CD43, CD44, and ICAM-2 (Legg and Isacke, 1998; Yonemura *et al.*, 1998). Therefore, instead of binding to α-actinin, this motif may also serve as a binding site for ERM proteins. Importantly, we found that RKIKK is a critical motif for the binding of ezrin, as determined by immunoprecipitation.

The important questions raised at this point are as follows: 1) What is a functional consequence of ICAM-1 localization on the microvilli? 2) Does microvillar elongation by ICAM-1 have any effect on leukocyte transmigration? and if so 3) What is the primary mechanism by which the spatial and physical distribution of ICAM-1 affects leukocyte transmigration across the endothelial cells? During leukocyte adhesion onto endothelial cells, ICAM-1 is rapidly relocalized to the newly formed membrane projection that is later known as a functionally important architecture for the para- and transcellular migration of leukocytes (Barreiro *et al.*, 2002; Carman *et al.*, 2003; Carman and Springer, 2004). Of particular importance, in the present results (Figure 7), dramatic reduction of membrane projection in mutant ICAM-1 lacking RKIKK strongly demonstrates that RKIKK is a critical motif for the ICAM-1 in connecting intracellular domain to the cytoskeletons and signaling networks. In agreement with this observation, a previous report demonstrated that membrane projections require intact microfilaments, microtubules, and calcium signaling (Carman *et al.*, 2003). To better understand the role of the microvillus presentation of ICAM-1 in physiological condition, we measured the leukocyte adhesion and migration under shear flow. Interestingly, leukocytes that adhered onto COS-7 wt-IC1 underwent dramatic shape changes and represented a flattened morphology. This shape change may help leukocytes to migrate on or across monolayers of endothelial cells under shear stress although the detailed mechanism is not determined in our present study. Because it has been demonstrated that rapidly migrating T lymphocytes form clustering of LFA-1 called "focal zone" in the midcell zone (Smith *et al.*, 2005), it could be possible that the microvillus presentation of ICAM-1 may facilitate focal zone induction, thereby sup-

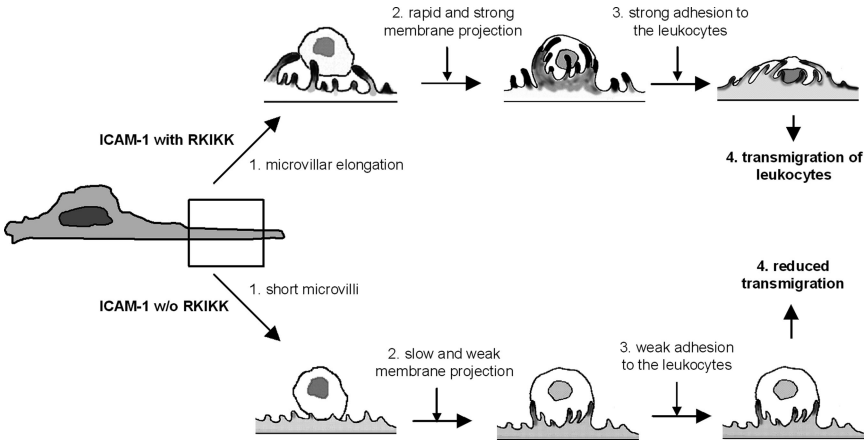

Figure 11. The proposed model of leukocyte adhesion on and transmigration through endothelial cells. The PKIKK motif in the intracellular domain plays a critical role not only for the physical distribution of ICAM-1 on the microvilli but also for the microvillar elongation by its potential interaction with ERM proteins and actin filaments. This spatial and dynamic organization provides a temporal docking site for adhesion and migration of activated leukocytes. This structure may also induce leukocyte shape changes and in turn triggers migration on or across monolayers of endothelial cells under the blood shear force.

porting leukocyte migration under shear stress. The shape change became noticeably more prominent when the leukocytes were loaded on the TNF-α–activated primary endothelial cells. This could be because of the multiple adhesion receptors expressed on endothelial cells. After binding to the endothelial cells, most leukocytes rapidly changed their morphology and induced ICAM-1 redistribution together with the enhanced transmigration.

In summary, the current findings show that an intracellular domain is important for the spatial and dynamic distribution of ICAM-1 on the cell surface. Importantly, the RKIKK motif in the intracellular domain plays a critical role not only for the physical distribution of ICAM-1 on the microvilli but also for microvillar elongation by its interaction with ERM proteins and actin filaments. This spatial and dynamic organization provides a temporal docking site for the adhesion and migration of activated leukocytes. Based on the findings in this report, a putative sequence of leukocyte binding to activated endothelial cells is schematically depicted in Figure 11. Although some reports have suggested a functional role of the intracellular domain in mediating inside signaling cascades through phosphorylation or induction of such signaling molecules as FAX, paxillin, $p130^{cas}$, and Rho (Etienne *et al.*, 1998; Adamson *et al.*, 1999), this is the first documented demonstration that the intracellular domain, especially the RKIKK motif, of ICAM-1 plays a critical role in leukocyte diapedesis.

ACKNOWLEDGMENTS

We thank Dr. Young-Myeong Kim (Kangwon National University, Chuncheon, Korea) for the supply of the primary HUVECs. We also thank Bonnie Hami (Boston, MA) for editorial assistance. This work was supported by grants from the Basic Research Program (R01-2005-000-10103-0) of the Korea Science and Engineering Foundation and from the Molecular and Cellular BioDiscovery Research Program (2006-02516) grant from the Ministry of Science and Technology, South Korea.

REFERENCES

Adamson, P., Etienne, S., Couraud, P. O., Calder, V., and Greenwood, J. (1999). Lymphocyte migration through brain endothelial cell monolayers involves signaling through endothelial ICAM-1 via a rho-dependent pathway. J. Immunol. *162*, 2964–2973.

Amieva, M. R., Litman, P., Huang, L., Ichimaru, E., and Furthmayr, H. (1999). Disruption of dynamic cell surface architecture of NIH3T3 fibroblasts by the N-terminal domains of moesin and ezrin: in vivo imaging with GFP fusion proteins. J. Cell Sci. *112*(Pt 1), 111–125.

Barreiro, O., Yanez-Mo, M., Serrador, J. M., Montoya, M. C., Vicente-Manzanares, M., Tejedor, R., Furthmayr, H., and Sanchez-Madrid, F. (2002). Dynamic interaction of VCAM-1 and ICAM-1 with moesin and ezrin in a novel endothelial docking structure for adherent leukocytes. J. Cell Biol. *157*, 1233–1245.

Carlos, T. M., and Harlan, J. M. (1994). Leukocyte-endothelial adhesion molecules. Blood *84*, 2068–2101.

Carman, C. V., Jun, C. D., Salas, A., and Springer, T. A. (2003). Endothelial cells proactively form microvilli-like membrane projections upon intercellular adhesion molecule 1 engagement of leukocyte LFA-1. J. Immunol. *171*, 6135–6144.

Carman, C. V., and Springer, T. A. (2004). A transmigratory cup in leukocyte diapedesis both through individual vascular endothelial cells and between them. J. Cell Biol. *167*, 377–388.

Carpen, O., Pallai, P., Staunton, D. E., and Springer, T. A. (1992). Association of intercellular adhesion molecule-1 (ICAM-1) with actin-containing cytoskeleton and alpha-actinin. J. Cell Biol. *118*, 1223–1234.

Casasnovas, J. M., Stehle, T., Liu, J. H., Wang, J. H., and Springer, T. A. (1998). A dimeric crystal structure for the N-terminal two domains of intercellular adhesion molecule-1. Proc. Natl. Acad. Sci. USA *95*, 4134–4139.

Durieu-Trautmann, O., Chaverot, N., Cazaubon, S., Strosberg, A. D., and Couraud, P. O. (1994). Intercellular adhesion molecule 1 activation induces tyrosine phosphorylation of the cytoskeleton-associated protein cortactin in brain microvessel endothelial cells. J. Biol. Chem. *269*, 12536–12540.

Dustin, M. L., and Springer, T. A. (1988). Lymphocyte function-associated antigen-1 (LFA-1) interaction with intercellular adhesion molecule-1 (ICAM-1) is one of at least three mechanisms for lymphocyte adhesion to cultured endothelial cells. J. Cell Biol. *107*, 321–331.

Etienne, S., Adamson, P., Greenwood, J., Strosberg, A. D., Cazaubon, S., and Couraud, P. O. (1998). ICAM-1 signaling pathways associated with Rho activation in microvascular brain endothelial cells. J. Immunol. *161*, 5755–5761.

Federici, C., Camoin, L., Hattab, M., Strosberg, A. D., and Couraud, P. O. (1996). Association of the cytoplasmic domain of intercellular-adhesion molecule-1 with glyceraldehyde-3-phosphate dehydrogenase and beta-tubulin. Eur. J. Biochem. *238*, 173–180.

Friederich, E., Huet, C., Arpin, M., and Louvard, D. (1989). Villin induces microvilli growth and actin redistribution in transfected fibroblasts. Cell *59*, 461–475.

Gaglia, J. L., Mattoo, A., Greenfield, E. A., Freeman, G. J., and Kuchroo, V. K. (2001). Characterization of endogenous Chinese hamster ovary cell surface molecules that mediate T cell costimulation. Cell. Immunol. *213*, 83–93.

Greenwood, J., Amos, C. L., Walters, C. E., Couraud, P. O., Lyck, R., Engelhardt, B., and Adamson, P. (2003). Intracellular domain of brain endothelial intercellular adhesion molecule-1 is essential for T lymphocyte-mediated signaling and migration. J. Immunol. *171*, 2099–2108.

Hall, H., Williams, E. J., Moore, S. E., Walsh, F. S., Prochiantz, A., and Doherty, P. (1996). Inhibition of FGF-stimulated phosphatidylinositol hydrolysis and neurite outgrowth by a cell-membrane permeable phosphopeptide. Curr. Biol. *6*, 580–587.

Heiska, L., Alfthan, K., Gronholm, M., Vilja, P., Vaheri, A., and Carpen, O. (1998). Association of ezrin with intercellular adhesion molecule-1 and -2 (ICAM-1 and ICAM-2). Regulation by phosphatidylinositol 4, 5-bisphosphate. J. Biol. Chem. *273*, 21893–21900.

Jun, C. D., Carman, C. V., Redick, S. D., Shimaoka, M., Erickson, H. P., and Springer, T. A. (2001a). Ultrastructure and function of dimeric, soluble intercellular adhesion molecule-1 (ICAM-1). J. Biol. Chem. *276*, 29019–29027.

Jun, C. D., Shimaoka, M., Carman, C. V., Takagi, J., and Springer, T. A. (2001b). Dimerization and the effectiveness of ICAM-1 in mediating LFA-1-dependent adhesion. Proc. Natl. Acad. Sci. USA *98*, 6830–6835.

Legg, J. W., and Isacke, C. M. (1998). Identification and functional analysis of the ezrin-binding site in the hyaluronan receptor, CD44. Curr. Biol. *8*, 705–708.

Male, D., Rahman, J., Pryce, G., Tamatani, T., and Miyasaka, M. (1994). Lymphocyte migration into the CNS modelled in vitro: roles of LFA-1, ICAM-1 and VLA-4. Immunology *81*, 366–372.

Miller, J., Knorr, R., Ferrone, M., Houdei, R., Carron, C. P., and Dustin, M. L. (1995). Intercellular adhesion molecule-1 dimerization and its consequences for adhesion mediated by lymphocyte function associated-1. J. Exp. Med. *182*, 1231–1241.

Reilly, P. L., Woska, J. R., Jr., Jeanfavre, D. D., McNally, E., Rothlein, R., and Bormann, B. J. (1995). The native structure of intercellular adhesion molecule-1 (ICAM-1) is a dimer. Correlation with binding to LFA-1. J. Immunol. *155*, 529–532.

Sans, E., Delachanal, E., and Duperray, A. (2001). Analysis of the roles of ICAM-1 in neutrophil transmigration using a reconstituted mammalian cell expression model: implication of ICAM-1 cytoplasmic domain and Rho-dependent signaling pathway. J. Immunol. *166*, 544–551.

Shimaoka, M. *et al.* (2003). Structures of the alpha L I domain and its complex with ICAM-1 reveal a shape-shifting pathway for integrin regulation. Cell *112*, 99–111.

Smith, A., Carrasco, Y. R., Stanley, P., Kieffer, N., Batista, F. D., and Hogg, N. (2005). A talin-dependent LFA-1 focal zone is formed by rapidly migrating T lymphocytes. J. Cell Biol. *170*, 141–151.

Smith, C. W., Marlin, S. D., Rothlein, R., Toman, C., and Anderson, D. C. (1989). Cooperative interactions of LFA-1 and Mac-1 with intercellular adhesion molecule-1 in facilitating adherence and transendothelial migration of human neutrophils in vitro. J. Clin. Invest. *83*, 2008–2017.

Smith, C. W., Rothlein, R., Hughes, B. J., Mariscalco, M. M., Rudloff, H. E., Schmalstieg, F. C., and Anderson, D. C. (1988). Recognition of an endothelial determinant for CD 18-dependent human neutrophil adherence and transendothelial migration. J. Clin. Invest. *82*, 1746–1756.

Springer, T. A. (1994). Traffic signals for lymphocyte recirculation and leukocyte emigration: the multistep paradigm. Cell *76*, 301–314.

Thompson, P. W., Randi, A. M., and Ridley, A. J. (2002). Intercellular adhesion molecule (ICAM)-1, but not ICAM-2, activates RhoA and stimulates c-fos and rhoA transcription in endothelial cells. J. Immunol. *169*, 1007–1013.

Yang, Y., Jun, C. D., Liu, J. H., Zhang, R., Joachimiak, A., Springer, T. A., and Wang, J. H. (2004). Structural basis for dimerization of ICAM-1 on the cell surface. Mol. Cell *14*, 269–276.

Yonemura, S., Hirao, M., Doi, Y., Takahashi, N., Kondo, T., and Tsukita, S. (1998). Ezrin/radixin/moesin (ERM) proteins bind to a positively charged amino acid cluster in the juxta-membrane cytoplasmic domain of CD44, CD43, and ICAM-2. J. Cell Biol. *140*, 885–895.

Yonemura, S., and Tsukita, S. (1999). Direct involvement of ezrin/radixin/moesin (ERM)-binding membrane proteins in the organization of microvilli in collaboration with activated ERM proteins. J. Cell Biol. *145*, 1497–1509.